


Article

Measurements of high-frequency Atmospheric Turbulence and its Impact on the Boundary Layer of Wind Turbine Blades

Alois Peter Schaffarczyk ¹  0000-0002-9357-3232 Andreas Jeromin ¹¹ Kiel University of Applied Sciences, Mech. Eng. Dept. Kiel, Germany; Alois.Schaffarczyk@FH-Kiel.de

* Correspondence: Alois.Schaffarczyk@FH-Kiel.de; Tel.: +49-431-210-2600

Abstract: To gain insight into the differences between onshore and offshore atmospheric turbulence, pressure fluctuations were measured for offshore wind under different environmental conditions. A durable piezo-electric sensor was used to sample turbulent pressure data at 50 kHz. Offshore measurements were performed at 100 m height on Germany's FINO3 offshore platform in the German Bight together with additional meteorological data provided by Deutscher Wetterdienst (DWD). The statistical evaluation revealed that the stability state in the atmospheric boundary has a large impact on turbulent fluctuations. Therefore, we used higher statistical properties (described by so-called shape factors) to the stability state. Data was classified to be either within the unstable, neutral or stable stratification. We found that in case of stable stratification, the shape factor is mostly close to zero, indicating that a thermally stable environment produces closer-to Gaussian distributions. Non-Gaussian distributions were found in unstable and neutral boundary layer states and an occurrence probability was estimated. Possible impact on laminar-turbulent transition on the blade is discussed with application of so-called laminar airfoils on wind turbine blades. Use of a cut-off frequency to separate load and aerodynamic turbulence is proposed.

Keywords: Advanced turbulence statistics, piezo-electric flow sensor, atmospheric boundary layer stability, laminar-turbulent transition

1. Introduction

Wind-energy was very successful during the last decades [1] to reach for a nearly stable annual investment corresponding to 50 GW rated power world-wide. This was in connection and in parallel to an impressive development in Wind Turbine Aerodynamics [2].

Due to this high number of annual installations, site assessment for wind farms has become more and more important and sophisticated even under offshore conditions. Tailored wind turbine design becomes state-of-the-art. In most cases turbulence is treated in context of loads, and frequency ranges higher than a few Hertz are generally considered to be of no importance. However, this high frequency turbulence plays a significant role in laminar-to-turbulent transition inside the boundary layer of blades for airplanes [3,4] and wind turbines [5,6]. Due to the much higher drag of turbulent parts thereon, this may give rise to much less efficiency of wind turbines (in terms of c_p) as desired and a proper choice of airfoils is crucial.

Particularly, in this paper, these high-frequency turbulent statistics are studied with respect to higher order statistical moments in some detail. The shape factor according to [7] - giving estimates of the extent to which turbulent fluctuations diverge from Gaussian behavior - is of special interest.

Unlike to earlier investigations, the Non-Gaussianity of turbulent pressure fluctuations could not be linked to one of the more popular atmospheric parameters like Reynolds number based on Taylor's micro-scale [8], wind speed or other common parameter. Therefore, we propose to characterize our findings according to the stability of the atmospheric boundary layer in terms of Richardson's number. We have organized the paper as follows: Firstly, the measurement set-up is described together with an indication of the locations at which they were performed. Then we describe our procedure used for data processing. After that we present and discuss our findings and finally draw some conclusions.



Figure 1. Locations of test sites onshore (Kaiser-Wilhelm-Koog) and offshore (FINO3 platform) 80 km west of the island of Sylt. ©FEZ FH Kiel GmbH, Graphics: Bastian Barton

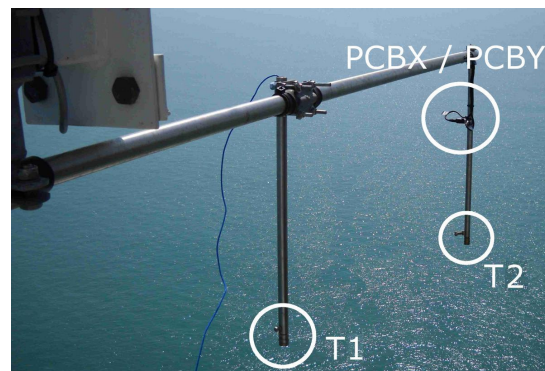


Figure 3. Installation of two parallel pressure sensors T1 and T2 at FINO3 platform

Parts of the material have been presented earlier in unpublished proceedings of ICCOWES2013 [9].

2. Measurements

Our first set of high-resolution measurements (during the years 2009 until 2011) were performed using piezoelectric pressure sensors from PCB Piezotronics (fig. 2) that was connected to an imc Meßsysteme GmbH CS-1208 data logger. The diameter of the sensing element was 12 mm. The minimal pressure resolution was 0.13 Pa, and the possible temporal resolution ranged from 2.5 Hz to 80,000 Hz. In [10] a correction method is proposed to increase the spacial resolution up to extension as large as three times the Taylor's length λ_T . As in our case we have values for λ_T ranging from 30 to 70 mm [8] we can be sure about the sensor's full resolution of 0.3 msec in time domain.

In our measurements the pressure data was sampled at 50 kHz with a total duration of 100 seconds. Wind speed and temperature were sampled at 1 Hz temporal resolution.

The piezoelectric pressure sensor was calibrated against a hot wire anemometer in a wind tunnel at University of Oldenburg. The turbulent wind speed from the hot wire anemometer and the turbulent pressure variations showed the same statistical properties up to 3 kHz [11].

Onshore measurements were conducted at the Kaiser-Wilhelm-Koog test site of Germanischer Lloyd/Garrad Hassan (see fig. 1). A lattice tower of 60 m height provided booms for mounting the

pressure sensor and other measurement equipment. The pressure sensor was mounted at 55 m height. Wind speed and wind direction were recorded at 55 m height by calibrated cup anemometers and wind vanes, respectively. The temperature was recorded at 53 m height by a resistor-type thermometer.

FEZ Kiel's platform FINO3 was the location for the offshore measurements. About 80 km west of the island of Sylt (see fig. 1) the platform was constructed close to no operational wind farms like DanTysk and Sandbank 24. The tower is a lattice tower type with booms of sufficient length for undisturbed measurements. Two pressure sensors (fig. 3) were mounted at about 100 m height above mean sea level for parallel operation. Data acquisition equipment for meteorological signals was similar to the equipment used onshore. Wind speed and wind direction were available at 100 m height, temperature at 95 m height above mean sea level.

3. Comparison with measurements from Laser Cantilever Anemometer

Usually, high frequency turbulence is measured with so-called hot-wire anemometers [12,13] with diameters down to a few micro-meters only. These small sensor extensions guarantee for high spacial and temporal resolution (if properly corrected for the **length** of the wire [10]) but the lifetime is restricted to few hours only. Therefore newly developed devices from University of Oldenburg, Germany, so-called Laser-Cantilever Anemometers (LCA) or special versions thereof, Atmospheric Laser-Cantilever Anemometers (ALCA) were used somewhat later [14–17]. Energy spectra agreed if \sqrt{p} was compared with v [11]. Unfortunately the design of the active sensor (30 μm X 35 μm X 9 μm in size) initially was spoiled with a resonance at about 1 kHz so that it had to be re-designed [18].

4. Analysis

Our recorded data sets were put into wind speed classes of 6 m/s, 12 m/s and 16 m/s. Measurements were triggered manually if wind conditions were regarded suitable. The bin sizes for each class are ± 2 m/s, for offshore class 10 m/s the upper bound was 11 m/s and for offshore class 12 m/s the lower bound was -1 m/s. For each measurement the statistical characteristics were analyzed with respect to power-spectral density, increment distributions, shape factor, structure functions, autocorrelation and Taylor's microscale.¹ We now explain our methods in more detail.

Increments of measured quantities are defined as usual:

$$\Delta u = u(t + \Delta t) - u(t) \quad \Leftrightarrow \quad \Delta p = p(t + \Delta t) - p(t) \quad (1)$$

where u is the velocity, p the pressure, t the time and Δt a fixed time delay. The increments also eliminate the mean value of the time series and thus stochastic fluctuations remain for a specific time scale Δt . These increments are our basic statistical quantities for more sophisticated analysis like structure functions or the so-called shape parameter.

[7] suggested that the distribution of increments may be described as an superposition of two distributions, one of them being lognormal. The shape factor then may be regarded as a measure of the level of intermittency. In Beck's approach from [20] the shape parameter can be calculated by 2nd and 4th order moments of the distribution:

$$s_u^2 = \ln \left(\frac{1}{3} \frac{\langle \Delta u^4 \rangle}{\langle \Delta u^2 \rangle^2} \right) \quad \Rightarrow \quad s_p^2 = \ln \left(\frac{1}{3} \frac{\langle \Delta p^4 \rangle}{\langle \Delta p^2 \rangle^2} \right). \quad (2)$$

¹ It may be interesting to note that Taylor's microscale may have a complementary interpretation in terms of a *Markov-Einstein coherence length* [19]. To us, this one seems to be much more physical than a somewhat vague interpretation in terms of an average turbulent vortex size

where s_u^2 is the shape factor for the velocity and s_p^2 for the pressure, respectively. The brackets $\langle x \rangle$ define the mean value of a quantity x . Further properties are given in [20]. A value of $s^2 \rightarrow 0$ indicates a normal distribution.

It is well-known at least since the work of [21] that turbulent velocities and pressure obey different scaling laws $\sim k^{-5/3}$ and $\sim k^{-7/5}$, respectively, although seemingly related by $p \sim v^2$ according to Bernoulli's law. Direct comparison of hot-wire with piezo-electric pressure sensor data show comparable power-density spectra up to 4 kHz (see [11], unpublished), however. Theoretical as well as experimental investigations of [22] are still incomplete, so that there is no clear answer so far about how s_u^2 and s_p^2 are related to each other exactly.

When heat transfer occurs, such as in the atmospheric boundary layer if the sea is warmer than the air (autumn), thermal stratification becomes more important. Simple static stability of the boundary layer may be used to characterize levels of turbulence. As was shown by [23], turbulence intensity differs remarkably for stable and unstable flow when used to describe fatigue loads of wind turbines.

A simple characterization of a stratified boundary layer exposed to heat transfer was introduced by [24] as belonging to a class consisting of stable, neutral or unstable states. Different calculation methods are used to distinguish these states ([24]) depending on what is known as input. In our case a Richardson's number approach was used. This one is defined as:

$$Ri = \frac{g}{T} \frac{\partial \theta / \partial z}{(\partial v / \partial z)^2} \quad (3)$$

where g is the acceleration of gravity, T is the mean absolute temperature, z is the height normal to the surface and $\partial v / \partial z$ is the mean velocity gradient. The z -direction is assumed to be vertical. A potential temperature θ is defined as

$$\theta = T \left(\frac{p_0}{p} \right)^{R/c_p} \quad (4)$$

where p is the pressure and $p_0 = 1000$ hPa the reference pressure, $R = 289 \frac{\text{J}}{\text{kg K}}$ is the specific gas constant and $c_p = 1005 \frac{\text{J}}{\text{kg K}}$ is the specific heat capacity of air.

In equation (3) the quantity $\frac{g}{T} \partial \theta / \partial z$ describes the forces introduced by heat transfer in the boundary layer. The term $(\partial v / \partial z)^2$ represents the momentum forces in the boundary layer. Now let us consider two points in the boundary layer at height z_1 and z_2 where $z_1 < z_2$ and $\Delta z = z_2 - z_1$. Ri from (3) can thus be rewritten with the differences between the two locations as

$$Ri = \frac{g}{T} \frac{\Delta \theta / \Delta z}{(\Delta v / \Delta z)^2} = \frac{g}{T} \frac{(\theta_2 - \theta_1) / \Delta z}{((v_2 - v_1) / \Delta z)^2} \quad (5)$$

We assume always positive velocity gradients so that only the convective part of Eq. (5) remains. Three typical situations then may be distinguished:

- $\theta_2 > \theta_1$ The surface is colder than the fluid and the gradient becomes $\partial \theta / \partial z > 0$ and therefore $Ri > 0$. Heat is transported by conduction only, and a convection flow does not occur. In this case the stratification is strong, and turbulence gets damped. The boundary condition is STABLE for $Ri > 0$.
- $\theta_2 = \theta_1$ The temperature gradient is zero and therefore $Ri = 0$. There is no temperature gradient and therefore no conduction nor convection. This condition is called NEUTRAL.
- $\theta_2 < \theta_1$ The surface is warmer than the fluid and the gradient becomes $\partial \theta / \partial z < 0$ and therefore $Ri < 0$. Heat is transported by conduction and by convection from the surface to the fluid. The convection results in a vertical, upward component of the flow that interacts with the horizontal velocity component. This leads to production of turbulence in the boundary layer and therefore is called UNSTABLE.

From our measurements we obtained the necessary values for p , T_{air} at 100 m height, wind speed v_{air} and wind direction as well as the sensor signal of the piezoelectric microphone. Assuming the air to be a perfect gas, the density ρ can be calculated by the perfect gas law.

For the derivatives $\partial\theta/\partial z$ and $\partial v/\partial z$, the temperature and wind speed at a second height must be known. Unfortunately, these data were not available during most of our measurements. Therefore, these gradients had to be approximated in a different way.

Ground temperature T_{gnd} was estimated using data from the Deutscher Wetterdienst (DWD). For the onshore measurements, the ground temperature at a nearby location was available at hourly samples. The temperature of the sea for the offshore measurements was interpolated from the measurement stations at the island of Helgoland and at List on the island of Sylt.

The sign of Ri mostly depends on the temperature gradient, so the velocity gradient can be regarded as of lower importance. Therefore, as a rough estimate $v_{gnd} \approx 0$ was used for our calculation of the velocity gradient. This effects mostly the absolute value of Ri but not the heat transfer conditions in the atmospheric boundary layer.

With this procedure estimates for Ri were possible. Identification of stable or unstable states was simple. However, the neutral state requires a value of exactly $Ri = 0$ which is difficult to attain precisely within our set of approximations. To indicate a nearly neutral state, a bandwidth of $|Ri| < 0.02$ was used instead.

5. Results

The computation of the shape parameter was straightforward, and the results are shown in figure 4. The scale for the shape factor is shown on the left. Colors indicate locations, and symbols represent velocity classes. Time series with $s_p^2 < 2$ were grayed out and will not be considered further in the following analysis. For purposes of comparison, shape factors from a particular velocity measurement ([12], $\bar{U}=7.6$ m/s, $u'=1.36$ m/s) was included (black line) as well.

The general behavior of both shape parameter functions for velocity and pressure is similar, whereas absolute values differ significantly. This behavior was also observed in [17]. Surprisingly, most of the pressure measurements resulted in s_p^2 close to zero.

Note the differences between the measurements of velocity and pressure concerning sampling rates and length of the time series.

In fig. 4 offshore curves were distinguished with numbers in brackets. They were all recorded on the same day with a short delay only:

- (1) October 19, 2010, 8:44 a.m.
- (2) October 19, 2010, 8:54 a.m.
- (3) October 19, 2010, 8:55 a.m.
- (4) October 19, 2010, 8:57 a.m.

Pressure time series were recorded for a period of 100 s. For the first data set (1) s_p^2 is high. But then the pressure data resulted in $s_p^2 \approx 0$ until the values increased eight minutes later at (2). The time series (2), (3) and (4) were consecutive, so it can be said that the shape parameter for the turbulent pressure fluctuations did not remain constant in time for this interval. When all time series from 8:44 to 8:57 were concentrated into one and evaluated according to a common s_p^2 , a curve similar to the curve for velocity fluctuations was obtained. This was already presented in [8].

We now try to relate these different statistical behavior to the atmospheric boundary layer state. With our estimation of the Richardson number a stability state was determined. Selected data from all our 119 measured data sets are shown in table 1. Measurements with $s_p^2 > 0$ are marked with a star in the last column.

As can be seen from table 1, high s_p^2 ($s_p^2 > 0$) behavior corresponds to unstable to neutral ABL conditions $-0.13 \leq Ri \leq 0.01$. However, a significant correlation with the Richardson number was not found.

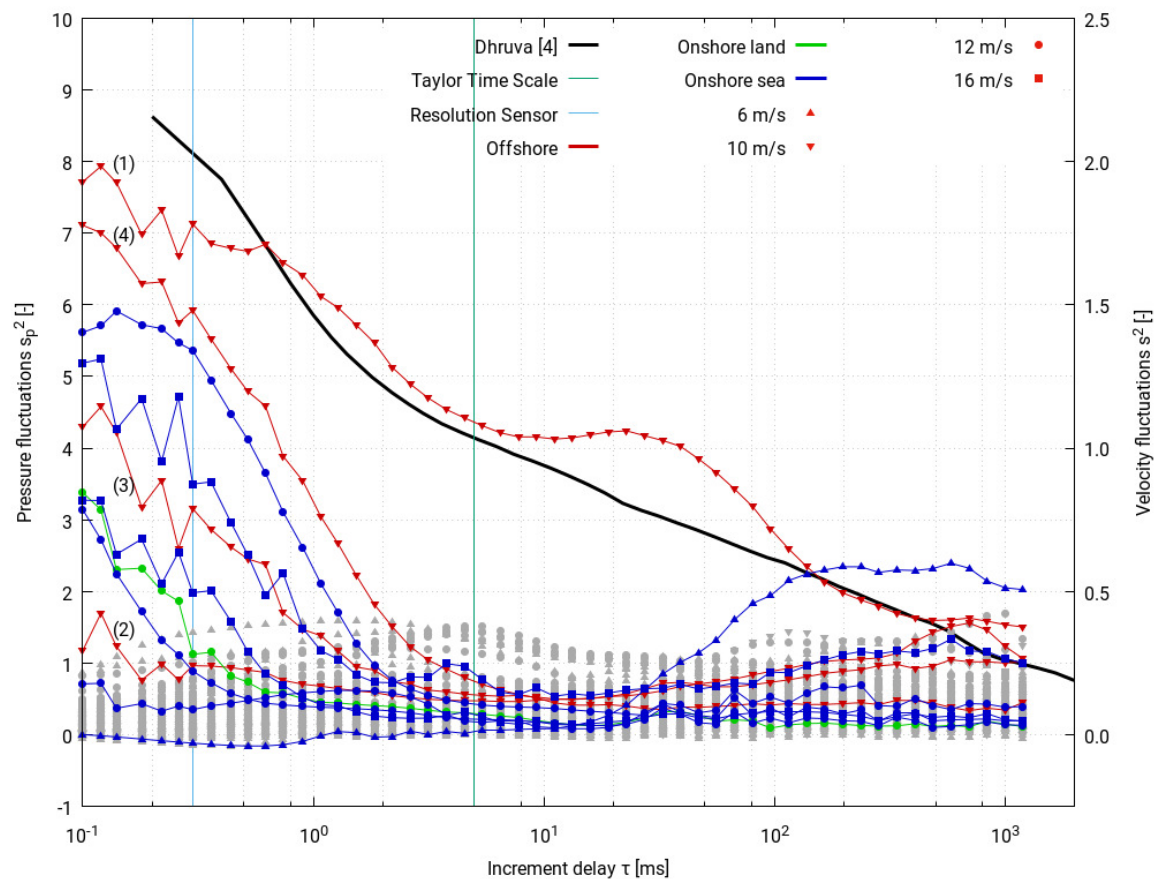


Figure 4. Shape parameters for all collected measurements. Colors represent locations: Offshore, Onshore with wind coming from land or sea side. Symbols represent the velocity classes for the wind speed. Measurements with $\max(s_p^2) < 2$ are in grey. For reasons of comparison Taylor's and Kolmogorov's time scales are given by 5 msec and 0.05 msec, resp. Sensor's resolution goes down to approximately 0.3 msec only.

5.1. Time Development of a Sample Time-Series

Therefore, for the measurement of Oct. 19, 2010 time variation of the shape factor was investigated in more detail. It is presented in table 2.

The measurement started at 8:44 a.m. when s_p^2 was high and the turbulence intensity from cup anemometers was low. In the following 7 minutes time series were found to have $s_p^2 \approx 0$, mean velocity and potential temperature of air remaining constant. Only turbulence intensity was increasing from about 4 to about 8 %.

At 8:54 a.m. the shape factor began to rise (see also curve (2) of fig. 4). Promptly, the turbulence intensity dropped more than 5.5 percentage points and also the potential temperature of the air decreased by 0.4 K with rising shape factor.

Our interpretation is summarized as follows: The Boundary Layer corresponding to time interval from 8:45 to 8:49 was stratified and turbulent pressure fluctuations were distributed in a Gaussian way. At 8:50 a.m. a cluster of warm air rose up from warmer sea-surface to higher (and colder) regions ($\theta_{air} \approx \text{const.}$, v_W fluctuating). This may have led to a stronger vertical shear thereby disturbing the (Gaussian) turbulent structures.

Table 1. Summary of selected ABL stability cases. Potential temperatures θ , wind speeds v_W and turbulence intensities Ti from cup anemometers, Ri numbers and estimated ABL state

Date & Time	Location	v_W (m/s)	Ti (%)	Ri (-)	Boundary layer state	
2010 Oct. 21, 7:56 a.m.	Offshore	6.6	8.2	-0.54	Unstable	
2008 Apr. 28, 9:35 a.m.	Onshore	6.1	11.9	-0.15	Unstable	
2010 Oct. 19, 8:57 a.m.	Offshore	10.8	2.2	-0.13	Unstable	*
2010 Oct. 19, 8:44 a.m.	Offshore	10.2	3.1	-0.12	Unstable	*
2010 Aug. 19, 8:13 a.m.	Offshore	12.7	2.8	-0.06	Unstable	
2008 Mar. 25, 2:55 p.m.	Onshore	11.3	10.8	-0.03	Unstable	*
2008 Mar. 29, 11:44 a.m.	Onshore	15.3	10.6	-0.01	Neutral	
2008 Mar. 30, 6:04 p.m.	Onshore	15.7	5.6	0.00	Neutral	*
2008 Apr. 28, 2:20 p.m.	Onshore	5.8	2.1	0.01	Neutral	*
2008 May 1, 2:55 a.m.	Onshore	6.0	6.0	0.10	Stable	
2008 Apr. 12, 7:24 p.m.	Onshore	5.2	11.0	0.28	Stable	

Table 2. Development of Time-Series on Oct 19. Potential temperatures θ , wind speeds v_W and turbulence intensities Ti from cup anemometers, Ri numbers and estimated ABL state

Time	θ_{air} (K)	θ_{gnd} (K)	v_W (m/s)	Ti (%)	Ri (-)	Boundary layer state	$s_p^2 \neq 0$
8:44 a.m.	283.6	286.8	10.2	3.1	-0.12	Unstable	*
8:45 a.m.	283.5	286.8	10.2	3.9	-0.13	Unstable	
8:47 a.m.	283.4	286.8	10.0	7.5	-0.14	Unstable	
8:49 a.m.	283.4	286.8	10.1	7.3	-0.13	Unstable	
8:50 a.m.	283.5	286.8	9.3	6.7	-0.16	Unstable	
8:52 a.m.	283.5	286.8	11.2	6.0	-0.11	Unstable	
8:54 a.m.	283.5	286.8	10.8	7.7	-0.11	Unstable	*
8:55 a.m.	283.2	286.8	11.2	4.2	-0.12	Unstable	*
8:57 a.m.	283.1	286.8	10.8	2.2	-0.13	Unstable	*

Table 3. Correlation of Occurrence-Probability of high shape-factor to boundary layer states for all 119 measurements

	Boundary layer state			Total
	Unstable	Neutral	Stable	
All	84	23	12	119
Offshore	65	0	0	65
Onshore	19	23	12	54
All $s_p^2 \neq 0$	7	4	0	11
Probability (%)	8	17	0	9
Offshore $s_p^2 \neq 0$	4	0	0	4
Probability (%)	6	-/-	-/-	-/-
Onshore $s_p^2 \neq 0$	3	4	0	7
Probability (%)	16	17	0	-/-

5.2. Occurrence probabilities

As was seen in our evaluations of boundary layer states and shape factor, occurrence of high values for s_p^2 (highly non-Gaussian behavior) seems to be connected to more sophisticated properties of the turbulent wind, which may be summarized by the term *intermittency*. These occurrence probabilities for all of our 119 measurements are listed in table 3.

In the first row the number of states are listed for all measurements. We see much more unstable (84) than neutral (23) or stable (12) conditions. The subsequent two rows list the numbers for offshore and onshore locations with their states. In the fourth row the tallies for high shape factor events were listed for all measurements. The probability for the occurrence of a high- s_p^2 event at a specific boundary layer state is shown in the next line. The same was done for both locations off- and onshore.

Notice that all measurements offshore were made during unstable conditions, while for the onshore measurements all three states were covered. This is due to the season when the experiments were performed. Onshore measurements took place in Spring 2008 between March and May. During this time of year ground begins to warm up only slowly while air heats up much faster. So, ground may be cooler than air and mainly stable states occur.

As our offshore measurements were performed mainly in late summer and autumn 2010, sea was still warmed-up by the summer season while air already started to cool down. Thus, mainly unstable conditions were covered by these sets of measurements.

To relate boundary layer state and the occurrence of high shape factors for the turbulent pressure fluctuations, the focus was placed on the onshore measurements. With a probability of about 16 % a high- s_p^2 was found for unstable and neutral states (tab. 3). But at stable conditions high- s_p^2 was not observed. So we conclude that turbulent fluctuations of the pressure may deviate from a normal distribution much more likely at unstable or neutral boundary conditions than at stable conditions.

5.3. Confidence considerations

To check the confidence of our above explanation, possible sources for errors were investigated. Individual measurements at onshore locations were recorded at different hours and days, so they could be assumed to be randomly sampled. Probability of occurrence of a high- s_p^2 event at unstable or neutral conditions was $\Phi_0 = 1/6$, tested by a binomial.

Let us state the hypothesis that the probability for a high- s_p^2 event in a stable state is the same as in unstable/neutral states. The hypothesis should be true, if one or more events occurred, and false, if no events occurred. For all twelve measurements at stable conditions this leads to a mean of 2 and a variance of 5/3. A possibility of no events was $P = 0.112 = 11\%$. So we can reject the hypothesis of identical probabilities with confidence of 89 %.

The confidence in the reliability of the assumed probability Φ_0 was checked. From the offshore measurements the probability for the occurrence of high- s_p^2 was estimated at $\Phi_1 = 0.06$. Let us

formulate the hypothesis that the probability Φ_0 is correct. And we also state the alternative hypothesis that the actual probability is indeed lower than Φ_0 , and the real probability for the occurrence of high- s_p^2 events is $\Phi_1 \approx 0.06$. The 42 onshore measurements were used as the set of random samples, and the hypothesis would be rejected when less than four high- s_p^2 -events occur. These assumptions lead to a probability of 6 %, where $\Phi_0 = 1/6$ would be assumed to be true, despite the fact it was wrong. Also, the probability Φ_0 might be rejected despite it was true with a probability of 24 %.

It could be concluded that onshore the probability for high- s_p^2 events was about 16 % with a confidence level of 94 %.

6. Impact on Boundary Layer Transition on a Wind Turbine Blade

In the preceding sections we have described that small-scale turbulence below Taylor's length-scale of less than 50 mm strongly shows non-Gaussian behavior. We now describe shortly how this may be related to turbulent-laminar transition on wind turbine blades. It has to be noted, that much more detailed investigations have been performed in the upper atmosphere for small aircrafts [3,4]. Corresponding field experiments on wind turbines were reported in [5,25]. From these, it can be concluded that despite high, integral turbulence intensity of more than 10 %, the energy content suitable for receptivity of TS-waves is even smaller than in a wind-tunnel environment. More evidence for a possible **low-frequency cut-off** for aerodynamically important turbulence can be given by a simple argument to estimate an **upper** frequency f^* for a boundary layer (BL) responding to an oscillating outer flow: Stokes [26], pp 191 ff, shows that an outer flow (oscillating with frequency ω) is damped out by viscosity according to $U = u_0 \cdot e^{-ky} \cdot \cos(\omega t - ky)$ with $k = \sqrt{\omega/2\nu}$, ν being the kinematical viscosity and U the main flow in x-direction and y being perpendicular to x . Now, if we introduce a *Stokes boundary layer thickness* by $\delta_S = 2\pi/k$ we reach for $f^* = 4\pi\nu/\delta^2 \approx 200$ Hz in our case. Here, we have set δ_S to an approximate value of 1 mm, a typical value for laminar boundary layers on airfoils at Reynolds numbers of several million. Therefore this high-frequency, non-Gaussian regime plays an important role in triggering TS-type of BL instability on the path to fully developed turbulence.

7. Conclusions

High-frequency - above 100 Hz - resolved measurements of pressure fluctuations for different average wind-velocities under on- and offshore conditions were investigated with respect to higher order statistical properties and were related to atmospheric boundary layer stability. It was found that up to 4 kHz pressure and velocity fluctuations obey the same power spectrum and further, that out of 119 time series in total some show high shape factors occurring with total probability of about 10 %, independent of Taylor-length based Reynolds-number. 64 % out of all high shape-factor events were recorded during unstable thermal stratifications and the level of occurrence seems to be almost doubled when compared to the on-shore case. If a continuous sequence of time series is investigated, strong variations of the shape factor are sometimes observed even during short periods of about half an hour.

As we argue for a separation of time-scales to distinguish between in-stationary and turbulent flow at about 100 Hz, it now becomes clear that a severe reduction of turbulence intensity takes place and explains why usage of laminar airfoils (NACA 63-215 for example) is meaningful.

Acknowledgments

We would like to thank the Germanischer Lloyd/Garrad Hassan (formerly WINDTEST) for their support during the measurement periods onshore as well as offshore. We thank the Department of Physics at the University of Oldenburg for their beneficial assessments and testing of our pressure sensors. Our thanks go also to the Deutscher Wetterdienst (DWD) for providing additional local temperature data. We thank the State of Schleswig-Holstein, Ministry of Science, Economics and Transportation for funding this project under Contract No. 122-09-023. Finally, we

acknowledge financial support by Land Schleswig-Holstein within the funding program Open Access Publikationsfonds.

Conflict of Interest

The authors declare no conflict of interest

- Schaffarczyk (Ed.), A. *Understanding WIND POWER TECHNOLOGY*; Wiley: Chichester, UK, 2014.
- A.P. Schaffarczyk. *Introduction to Wind Turbine Aerodynamics*; Springer Verlag, Berlin, 2014.
- A.D. Reeh and M. Weissmüller and C. Tropea. Free-Flight Investigation of Transition under Turbulent Conditions on a Laminar Wing Glove. 51st AIAA Aerospace Sciences Meeting, 2013.
- Reeh, A.D.; Tropea, C. Behaviour of a natural laminar flow airfoil in flight through atmospheric turbulence. *J. Fluid. Mech.* **2015**, *767*, 394–429.
- Schaffarczyk, A.; Schwab, D.; Breuer, M. Experimental Detection of Laminar-Turbulent Transition on a Rotating Wind Turbine Blade in the Free Atmosphere. *WIND ENERGY* **2016**, *19*, DOI 10.1002/we.2001.
- Schwab, D. Aerodynamische Grenzschichtuntersuchungen an einem Windturbinenblatt im Freifeld. PhD thesis, Helmut-Schmidt-Universität/ Universität der Bundeswehr, 2018.
- Castaing, B.; Gagne, Y.; Hopfinger, E. Velocity probability density functions of high Reynolds number turbulence. *Physica D* **1990**, *64*, 177–200.
- Jeromin, A.; Schaffarczyk, A.P. Advanced Statistical Analysis of High-Frequency Turbulent Pressure Fluctuations for On- and Off-shore Wind. EUROMECH Colloquium 528: Wind Energy and the impact of turbulence on the conversion process, Oldenburg, Germany, 2012.
- A. Jeromin and A. P. Schaffarczyk. Relating High-Frequency Offshore Turbulence Statistics to Boundary Layer Stability. Proceedings of the: 2013 International Conference on Aerodynamics of Offshore Wind Energy Systems and Wakes (ICOWES2013); Shen, W.Z., Ed., 2013, pp. 162–172.
- Segalini, A.; R., O.; Schlatter, P.; P.H., A.; Rüedi, J.D.; A., T. A method to estimate turbulent intensity and transvers Taylor microscale in turbulent flows from spatially averaged hot-wire data. *Exp. Fluids* **2011**, *51*, 693–700.
- Jeromin, A.; Schaffarczyk, A.P. Statistische Auswertungen turbulenter Druckfluktuationen auf der off-shore Messplattform FINO3. Technical Report unpublished internal Report No. 78, in German, University of Applied Sciences Kiel, 2012.
- Dhruva, B. An Experimental Study of High Reynolds Number Turbulence in the Atmosphere. PhD thesis, Yale University, USA, 2000.
- Sreenivasan, K.; Dhruva, B. Is There Scaling in High-Reynolds-Number Turbulence? *Pr. Theo.Phys. Supp.* **1998**, *130*, 103–120.
- Hölling, M. Sensorentwicklung für Turbulenzmessungen. PhD thesis, Carl von Ossietzky Universität Oldenburg, 2008.
- Puczyłowski, J. Sensor development for highly resolved measurements in turbulent flow. PhD thesis, Carl von Ossietzky Universität Oldenburg, 2015.
- Puczyłowski, J.; Hölling, A.; Peinke, J.; R., B.; Hölling, M. A new approach to highly resolved measurements of turbulent flow. *Meas. Sci. Technol.* **2015**, *26*, 055302.
- Jeromin, A.; Schaffarczyk, A.; Puczyłowski, J.; Peinke, J.; Hoelling, M. Highly resolved measurements of atmospheric turbulence with the new 2D-atmospheric Laser Cantilever Anemometer. The Science of Making Torque from Wind 2012; , 2012.
- Reichstein T. and Schaffarczyk, A.P. and Puczyłowski J. and Hölling M. and Stein D.. Measurements of the Atmospheric Turbulence with a customized 2D-ALCA. Proc. DEWEK 2017, 2017.
- Lück, S.; Renner, Ch., P.J.; R., F. The Markov-Einstein coherence length - an new meaning for the Taylor length in turbulence. *Phys. Lett.* **2006**.
- Beck, C. Superstatistics in hydrodynamic turbulence. *Physica D* **2004**, *193*, 195–207.
- Batchelor, G. Pressure fluctuations in isotropic turbulence. *Proc. Cam. Phil. Soc* **1951**, *47*, 359–374.
- Xu, H.; Ouellette, T.; Vincenzi, D.; Bodenschatz, B. Acceleration Correlations and Pressure Structure Functions in High-Reynolds Number Turbulence. *Phys. Rev. Lett.* **2007**, *99*, 204501,1–4.

23. Sathe, M.; Mann, J.; Barlas, T.; Bierbooms, W.; van Bussel, G. Influence of atmospheric stability on wind turbine loads. *The Science of Making Torque from Wind*; , 2012.
24. Obukhov, A.M. Turbulence in an Atmosphere with a Non-Uniform Temperature. *Boundary-Layer Metereology* **1971**, 2, 7–29.
25. H. Aa. Madsen et al. The DAN-AERO MW experiments. *AIAA* **2010**, 2010-645, 1–13.
26. Batchelor, G. *An Introduction to Fluid Dynamics*; Cambridge University Press: Cambridge, UK, 1967.

Nomenclature

Abbreviations

ALCA Atmospheric Laser-Cantileaver Anemometer

FEZ Forschungszentrum FH Kiel GmbH (Research Center of Kiel University of Applied Sciences, Ltd.)

FINO Forschung in Nord- und Ostsee (Research at North and Baltic Sea)

LCA Laser-Cantileaver Anemometer

NACA National Advisory Committee of Aeronautics

Variables

s_p Shape factor for pressure

k Turbulent kinetic energy

p static pressure

u Velocity in main (x) direction